

Passenger Flow Prediction of Tourist Attractions by Integrating Differential Evolution and GWO

Jie Yu

Modern Service College, Zhengzhou Tourism College, Zhengzhou 451464, China

E-mail: gracefish_83@163.com

Keywords: time series, GWO algorithm, LSTM network, differential evolution algorithm, traffic prediction, travel

Received: May 7, 2024

To further improve the experience of visiting tourist attractions and promote their long-term healthy development, this study analyzes the short-term passenger flow prediction of tourist attractions. The traditional long and short-term memory network is selected as the basis of the prediction framework. Then the grey wolf optimization algorithm is used to optimize the hyper-parameters of the long and short-term memory network, and the differential evolution algorithm is used to improve the shortcomings of easily falling into the local optimum. Finally, a passenger flow prediction model is constructed based on intelligent optimization and deep learning. The experiment outcomes denote that the differential evolution improvement strategy designed in the study is beneficial for improving the global optimization of the grey wolf evolutionary algorithm. The average optimization values of different test functions are closest to the global minimum, effectively improving the population fitness. In the parameter optimization, the maximum value of hypervolume can reach 0.91. The minimum value of the inverse generation distance converges to 0.09, and the quality of the Pareto front solution is relatively high. The Spacing and Spread values are both above 0.8, indicating better diversity in the solution set. The improved prediction model has the lowest values in terms of mean absolute percentage error, root mean square error, and mean absolute error, and the minimum value of the error is only 0.0693. The maximum R2 value can reach 0.945, indicating good prediction accuracy and goodness of fit. The prediction results of this prediction model have high accuracy in predicting passenger flow at different time periods. The accuracy and F1 values are close to 0.95 and the precision and recall are higher than 0.90 on different datasets. This study enriches the theoretical basis for optimizing and improving traditional time series models, improves the accuracy of predicting tourist flow in tourist attractions, and helps promote the healthy development of the tourism industry.

Povzetek: Predstavljen je sistem za napovedovanje potniškega toka turističnih znamenitosti, ki združuje diferencialno evolucijo in optimizacijski algoritem sivega volka (GWO) z LSTM mrežo. Model dosega visoko točnost napovedi s povprečnim R^2 do 0,945, kar prispeva k izboljšanju načrtovanja turističnih obiskov in razvoju turizma.

1 Introduction

With the transformation and upgrading of the national industrial structure, the tourism industry takes a pivotal part in economic development. The tourism industry has emerged as a significant contributor to regional economic development, bringing in a large amount of economic income while also driving the development of other related industries [1]. But with the booming development of the tourism, the passenger flow of tourist attractions (TAs) continues to increase. Moreover, travelers are mostly concentrated at holiday nodes, leading to an imbalance in the allocation of tourism resources in terms of time and space. These types of problems seriously interfere with the safety management of scenic spots, affect the travel experience of tourists, and bring negative impacts to the development of TAs [2-3]. Thus, it is significant to forecast the passenger flow data of TAs

through effective methods, help scenic spots to make reasonable planning and adjustments in resource allocation, personnel allocation, service quality, etc., formulate reasonable flow limiting measures to avoid overcrowding and resource waste, and promote the long-term sustainable development of the tourism [4]. At present, research on predicting the passenger flow of TAs mostly comes from the analysis of annual and monthly tourism data, and the prediction results have a strong lag, making it difficult to provide effective and reasonable guidance for scenic area management and tourist travel [5-6]. Today, in the context of "Internet plus", advanced computer, big data and other technologies and information systems have greatly promoted the upgrading and transformation of intelligence and informatization of tourism. However, the management of smart tourism services is still in the exploratory stage, and the construction of technology and infrastructure still needs

to be further strengthened [7-8]. In view of this, to further enhance the intelligence and scientificity of tourism industry management, deep learning algorithms are introduced into the problem of tourism passenger flow prediction (PFP), and a corresponding framework is built grounded on long and short-term memory networks (LSTM). Moreover, the grey wolf optimization (GWO) algorithm is introduced to optimize the hyperparameters of LSTM. The introduction of differential evolution (DE) algorithm during the optimization improves the shortcomings of GWO.

The innovation of the research is mainly reflected in three aspects. Firstly, it further improves the level of intelligent management in the tourism industry. Secondly, it enriches the theoretical research level of time series prediction models and introduces intelligent optimization algorithms (IOAs) to achieve parameter optimization. Thirdly, it expands the application fields and potential of IOAs. The research is broken into four parts. Part 1 illustrates the current research conditions of prediction problems and IOAs. Part 2 constructs a PFP model with LSTM. Part 3 conducts testing experiments on the effectiveness of the prediction model. The fourth part summarizes the main conclusions of the study and future work. This study is expected to strengthen the intelligence level of the entire tourism industry management and enrich the travel experience of tourists.

2 Related works

Predictive research is related to decision-making problems in many fields and is an important research direction in computer and artificial intelligence, receiving widespread attention from scholars. At present, the traffic prediction methods for TAs are mostly limited to raw traffic data and road networks. Gao et al. comprehensively considered the urban road network, scenic spot popularity, accessibility, and traffic volume, and used multiple historical data sources to learn the traffic dependence of multiple scenic spots through multi-graph convolutional networks and gated recurrent units for TAs traffic volume prediction. The experimental results indicated that the model can utilize integrated data for traffic flow prediction [9]. Holiday tourism requirement prediction is a critical part of the tourism transportation system's planning and management. Li et al. designed an improved spatiotemporal related LSTM model to predicate tourism demand by combining the spatiotemporal related history of passenger flow, weather, time, Internet search index and other data. Empirical analysis and verification of actual passenger flow data in suburban TAs in Beijing indicated that in contrast with other conventional prediction models, this model has better ability to capture spatiotemporal correlation of traffic flow and higher prediction accuracy [10]. The existing solutions for PFP are mostly based on regional prediction, with limited prediction capabilities. Sáenz et al. constructed a prediction framework based on graph

neural networks, which integrates multi-source heterogeneous tourism data related to national mobility and infrastructure characteristics. The graph neural network was integrated into the graph model, and the experiment findings indicated that the model's F1 value was higher than 0.7 [11]. Short-term PFP is the key to the operation and scheduling decisions of urban rail transit. To avoid potential threats caused by massive passenger flows, Xu conducted PFP research on the subway system and designed a multi-stage urban rail transit short-term PFP model that integrates convolutional neural networks, LSTM, support vector machines, and wavelet transform. The experimental outcomes indicated that the integrated model is superior to the baseline model in accuracy and efficiency, and the values of various error evaluation indicators are better than classical prediction techniques [12].

The spatial clustering of tourist quantity sequences limits the accuracy of tourist flow prediction models. Xue et al. designed a multimodal deep learning method for predicting hourly tourist flow in scenic spots based on spatial aggregation. This method effectively utilized search engine data to extract daily features of scenic spots, and utilized social media and tourist quantity data to explore spatial aggregation relationships. The empirical results showed that this method is superior to existing advanced baseline models, with a significance level of 1%. Compared with the optimal baseline model, this method achieved a maximum reduction of 50.0% in error values [13]. To provide better personalized itinerary management for TAs and effectively avoid peak travel hours, Sun et al. designed a convolutional block attention module with deep learning for predicting tourism demand. This method first extracted a passenger flow grid graph from mobile signaling data, then constructed a convolutional block attention module using a multi-channel spatiotemporal grid graph constructed from multiple continuous passenger flow grid graphs, and finally predicted the demand for TAs. The findings of the experiment indicated that the mean absolute percentage error (MAPE) of this method is 8.11%, which is superior to that of other deep learning models [14].

IOA is a type of solving algorithm based on natural phenomena and biological inspiration, and different intelligent algorithms are broadly applied in different fields. Lu et al. conducted research on the optimization analysis of genetic algorithm, particle swarm optimization (PSO) algorithm, GWO algorithm, and sparrow search algorithm (SSA), in support vector regression. The optimized machine learning method was used to forecast the geological displacement generated by tunnel excavation. The fitness function analysis results showed that the GWO algorithm and SSA have high accuracy, efficiency, and stability [15]. Wang et al. designed a new multi-objective marine predator combination strategy for wind speed combination probability prediction. The experiment outcomes indicated that this method overcomes the deficiencies of

traditional multi-objective optimization algorithms and effectively measured and minimized the uncertainty in the prediction process [16]. To predict the uniaxial compressive strength of the novel rubber sand concrete material, Mei et al. selected PSO, fruit fly optimization, lion swarm optimization, and SSA to enhance the backpropagation neural network. The verification results of six performance evaluation indicators showed that the lion swarm optimization algorithm had the best performance [17]. Abdullaev et al. optimized the customer churn prediction model based on bidirectional LSTM using the chicken swarm optimization algorithm. Experiment outcomes indicated that the optimized prediction model performs better than other prediction techniques [18]. To improve the problem of poor trajectory accuracy and susceptibility to local optima in inland ship trajectory prediction models, Zheng Y et al. improved the SSA using sine chaotic mapping and utilized it to strengthen the weight and threshold of the prediction model. Experiment outcomes indicated that

this method improves the prediction model’s accuracy and stability [19].

In summary, both domestically and internationally, the PFP in TAs mainly relies on traditional time series models, machine learning algorithms, or deep learning algorithms, and the prediction problem has made good research progress. The main methodology, dataset, assessment indicators and key findings of the study are shown in Table 1. However, these classic time series prediction methods require a large amount of computation and a longer training time. There is still some room for improvement in the model's predictors. At present, IOAs have been widely used for optimizing various model parameters or solution spaces, the use of IOAs to improve the performance of prediction models has become a popular trend, and the problem of tourism traffic prediction needs to be solved. Moreover, research also attempts to introduce IOAs to raise the performance of traditional time series prediction models.

Table 1: Summary of existing research reviews

Literature	Main methods	Dataset	Evaluation indicators	Main conclusions
[9]	Graph convolutional network, gated recurrent unit	Integrate geographic data and historical traffic data	Accuracy	The prediction accuracy is better than several classical and recent methods
[10]	An improved spatiotemporal correlation LSTM model	Historical data of the tourist flows, and the auxiliary data including meteorological data, temporal data, and Internet search index	Prediction accuracy	Better ability to capture spatiotemporal correlation of flow with higher prediction accuracy
[11]	Graph neural network	Heterogeneous tourism data	F1 value	F1 value above 0.7
[12]	Integrated convolutional neural network, LSTM, support vector machine and wavelet transform	Historical data of urban subway system	MAPE, RMSE, mean square error, R ² , and accuracy	The prediction model is better than the baseline model in accuracy and efficiency, and the evaluation index is better than the classical prediction technology

[13]	Multimodal deep learning methods	Real-time tourist quantity dataset for different scenic spots in Beijing	MAPE, RMSE	The Diebold Mariano test is superior to state-of-the-art baseline models at the 1% level, with significantly reduced error values
[14]	Deep learning model based on convolutional block attention module	Beijing and Xiamen mobile signaling data	MAPE	The MAPE of this method is 8.11%, which is better than other deep learning models
[15]	Genetic algorithm, PSO, GWO and SSA optimize the machine learning prediction model	Soil pressure balance shield tunnel excavation construction data	Pearson correlation coefficient	The GWO algorithm and SSA have high accuracy, efficiency, and stability
[16]	Combined probability prediction of wind speed based on multi-target marine predator combination strategy	Two wind speed data sets	Prediction accuracy	Improve wind speed prediction accuracy, effectively measure and minimize forecast uncertainties
[17]	PSO, fruit fly optimization, lion swarm optimization, and SSA to enhance the backpropagation neural network	Uniaxial compression test data from RSC laboratory	RMSE, correlation coefficient, coefficient of determination, MAE, mean square error, and sum of squares of error	Lion swarm optimization enhance the backpropagation neural network better than the other three mixed models
[18]	Bidirectional LSTM prediction model based on chicken flock optimization algorithm	Customer information data set	/	The performance is better than other prediction techniques
[19]	Sinusoidal chaotic mapping improved SSA to optimize the prediction model	Data of ship automatic identification system in the Yangtze River	Accuracy and stability	This method improves the accuracy and stability of the prediction model

model framework, and introduces IOAs to optimize the model parameters.

3 A tourist flow prediction model for tourist attractions based on improved LSTM

Predicting the passenger flow of TAs helps optimize tourism products and services, improve tourist satisfaction and experience. The study selects LSTM from deep learning algorithms to construct a prediction

3.1 Distribution characteristics of passenger flow in tourist attractions and construction of LSTM prediction framework

The PFP of TAs can be broken into medium and long-term PFP and short-term PFP. Medium and long-term passenger flow refers to the number of tourists

over a relatively long period of time, usually evaluated based on the passenger flow of statistical years or quarters. It is influenced by factors such as economic conditions, scenic area facilities and service levels, and tourism policies. Short-term passenger flow refers to the passenger flow within a relatively short time range, usually daily, weekly, or monthly. It has many influencing factors and fluctuates greatly [20-21]. The study focuses on analyzing PFP, and the process of analyzing passenger flow characteristics and building a prediction framework is shown in Figure 1.

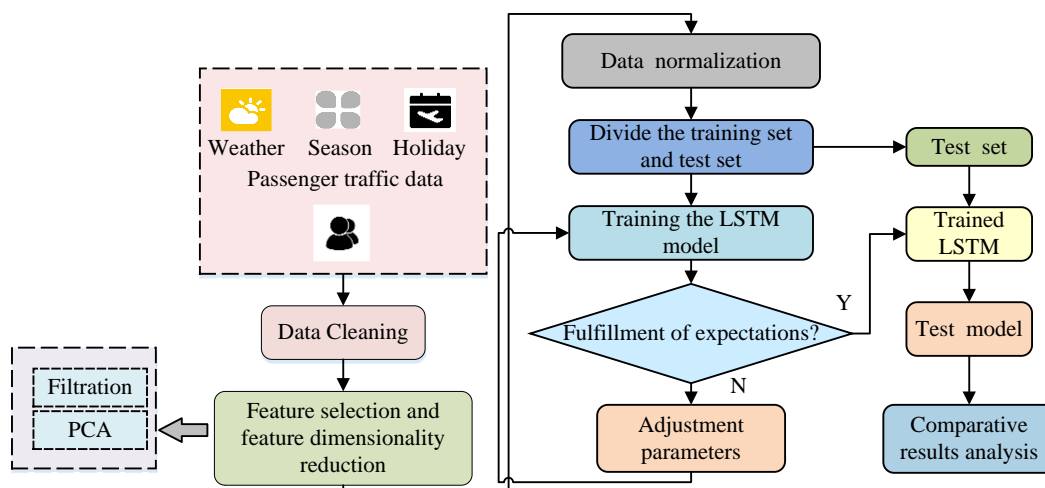


Figure 1: Flow of passenger traffic characterization and prediction framework construction

The study summarizes the influencing factors and distribution characteristics of tourist flow in TAs by reviewing relevant materials, literature, and yearbook reports related to scenic area management and passenger flow analysis. According to research, the main factors affecting tourist flow in TAs include weather, season and holiday influences, public opinion, and word-of-mouth. Factors such as weather comfort, rainfall, and temperature can affect the travel comfort of tourists. Under the current vacation system in China, holidays usually have a significant influence on the passenger flow of TAs. In addition, the promotion and publicity activities, positive public opinion, and good reputation of the scenic area will also attract tourists to travel. Overall analysis shows that the distribution characteristics of passenger flow in TAs are influenced by various factors, showing significant fluctuations during peak and valley periods. On weekends and holidays, the increase in passenger flow is more pronounced. Therefore, the passenger flow data has non-linear characteristics and obvious periodicity, showing differences between centralized distribution and decentralized distribution.

The influencing factors of passenger flow are collected, they are transformed into trainable predictive model features, and feature selection and dimensionality reduction are performed to reduce redundant information

between data, reduce data dimensions, and improve the model's generalization ability and interpretability. The feature selection method adopted in the study is the filtering method, which filters features by setting a threshold. The method employed for the reduction of dimensionality is principal component analysis (PCA). PCA applies the covariance matrix of data to map the original features to a new feature space, preserving the original information and reducing data correlation. The expression of the covariance matrix is shown in equation (1). In equation (1), m represents the feature dimension of the sample. x represents matrix elements.

$$\sum = \frac{1}{m} \sum_{i=1}^m x_i x_i^T \tag{1}$$

The study uses recurrent neural networks (RNNs) in deep learning as the technical foundation for prediction models. Traditional artificial neural networks rely on nonlinear mapping relationships to achieve predictive outputs, lacking the ability to capture the relationship between data and time. RNN is suitable for processing sequential data, memorizing the information learned during training, and applying it to the learning and computation of the current task. The network structure of RNN is denoted in Figure 2 [22].

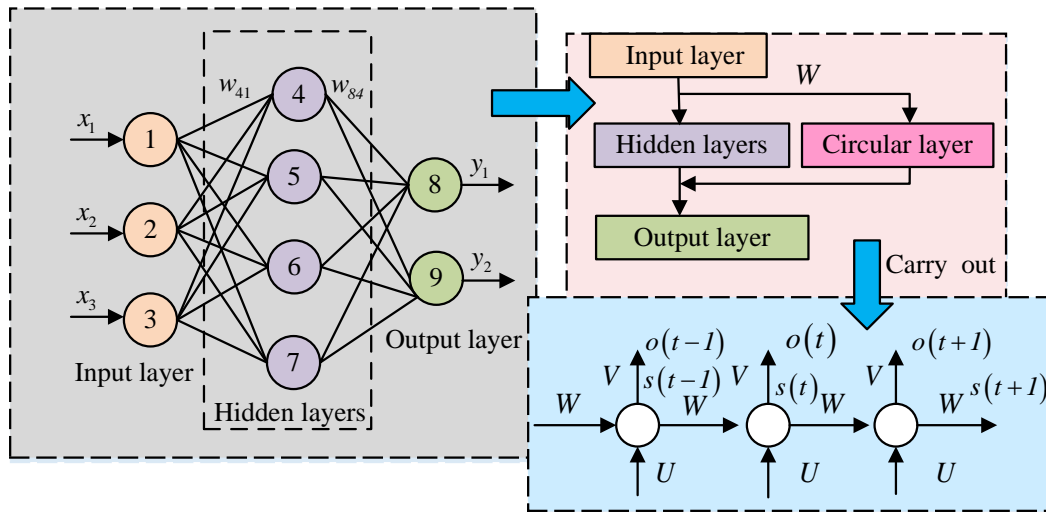


Figure 2: Schematic diagram of recurrent neural networks

After inputting the sequence data into the RNN, the hidden state is iteratively calculated at each time step, and the output is predicted with the hidden state. The nodes between the hidden layers (HLs) are interconnected and jointly determine the output of the next moment. The operation process of RNN is shown in equation (2), wherein $h(t)$ and $o(t)$ represent the outputs of the HL and output layer (OL), respectively. t represents a time series. $s(t)$ means the memory of the sample at time t . $f(\cdot)$ and $g(\cdot)$ represent nonlinear activation functions. $g(\cdot)$, W , V represent the weight matrices of input layer, HL, and OL, respectively.

$$\begin{cases} h(t) = Ux(t-1) + Ws(t-1) \\ s(t) = f(h(t)) \\ o(t) = g(Vs(t)) \end{cases} \quad (2)$$

The complexity of the structural composition of RNNs increases over time, and information is lost during

transmission. RNNs face problems such as vanishing or exploding gradients. To avoid such phenomena, the improved structure LSTM of RNN is used in the study [23]. LSTM replaces the hidden neurons of RNN with structures with LSTM, including memory cells, input gate (IG), output gate (OG), and forget gate (FG). The different parts control the memory and forgetting of information through learning parameters, thereby determining the updating of cell states and the calculation of hidden states. Among them, the FG determines the information forgotten from the cell state, the IG determines the addition of input data to the cell state, and the OG calculates the hidden state based on the current input and cell state [24]. Compared to RNN, LSTM can capture and retain important information, better handle long-term dependencies and long-range correlations in sequences. The schematic diagram of LSTM structure is denoted in Figure 3.

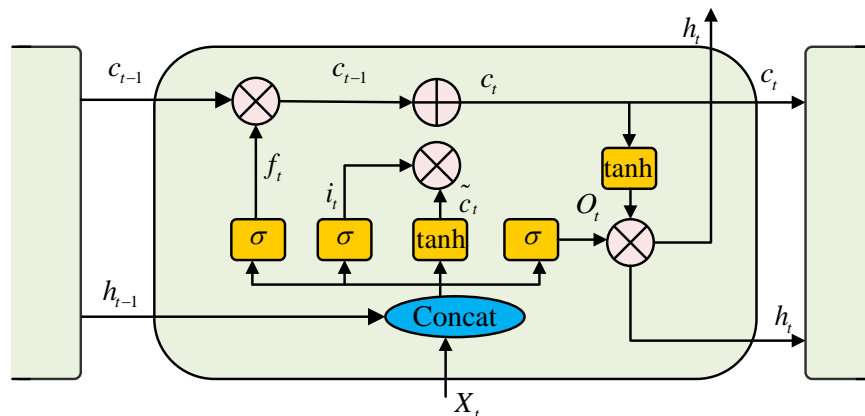


Figure 3: Schematic diagram of LSTM network

The expression for the internal state S_t and HL state y_t of LSTM is shown in equation (3). In equation (3), f_t , i_t , and O_t correspondingly denote FG, IG, and OG. S_t denotes the intermediate state of the current internal state.

$$\begin{cases} S_t = f_t \times S_{t-1} + i_t \times S_t \\ y_t = O_t \tanh(S_t) \end{cases} \quad (3)$$

The expression for the FG is shown in equation (4). In equation (4), W_f means the weight of the FG. b_f means forgetting gate bias. σ represents the activation function. The FG can effectively filter out abnormal and redundant data.

$$f_t = \sigma(W_f[y_{t-1}, x_t] + b_f) \quad (4)$$

The IG determines the addition of input data to the cell state, and the calculation process is denoted in equation (5). In equation (5), W_i , b_i , and W_o , b_o correspond to the weight matrix and bias of the IG and OG.

$$\begin{cases} i_t = \sigma(W_i[y_{t-1}, x_t] + b_i) \\ O_t = \sigma(W_o[y_{t-1}, x_t] + b_o) \end{cases} \quad (5)$$

3.2 Design of improved LSTM prediction model based on DE and GWO

Traditional LSTM networks involve the selection of many parameters, including the amount of HL nodes, initial learning rate, iteration times, etc. When the amount of HL nodes is small, the model cannot capture detailed patterns and relationships, which is prone to underfitting. When there are many HL nodes, it may lead to overfitting of the model. The size of the learning rate influences the speed and direction of network parameter updates, and affects the convergence ability of the model. The number of iterations is related to the model's learning of data features, which affects the model's fitting ability. In summary, the LSTM model involves many parameters, and the selection of parameters requires repeated training and adjustment based on actual tasks and data. To find reasonable and effective LSTM network parameters, the study chose to introduce GWO, an IOA, for hyperparameter optimization. Three hyperparameters, the number of HL nodes, the batch size and the initial value of the learning rate of the LSTM network, were selected for optimization. The range of the number of HL nodes was set to [1, 250], the range of the batch size was set to [1, 64], and the range of the initial value of the learning

rate was set to [0.001,0.5]. The hyperparameters obtained from intelligent optimization were input into the test set for validation, and the hyperparameters were considered optimal when the mean square error of the prediction model was minimized. The total number of parameters of LSTM network included IG, OG, FG and candidate state, and the parameters of LSTM were simplified into two matrices, which map the input and output respectively, one of which has the dimension of $hidden*input$, and the other has the dimension of $hidden*hidden$, and the total number of parameters was namely $4(hidden*input + hidden*hidden + hidden)$. The input feature dimension of the LSTM network is defined as n , the length of the input sequence as T , the dimension of the hidden state as m , and the time complexity of the LSTM network as $O(4Th^2 + 4Tnh)$. The introduction of the GWO algorithm will somewhat increase the computational complexity of the LSTM network.

The GWO algorithm is a natural heuristic algorithm that simulates the predatory social behavior of grey wolf groups. According to the mechanism of hunting cooperation in grey wolf groups, it achieves the goal of problem optimization and solution. GWO has been widely used in neural network optimization, various scheduling, control, and combination problem solving. Compared to other optimization algorithms, GWO possesses the following attributes: simplicity, ease of implementation, robust global search capabilities, and rapid convergence speed. [25-26].

Usually, there is a strict hierarchical system in a grey wolf pack, which is generally divided into four levels: first-level α , second-level β , third-level δ , and fourth-level ω . Based on the hierarchy of the grey wolf pack, high-level grey wolves have absolute dominance over low-level grey wolves. When designing GWO models, it is necessary to first construct a hierarchical model of the grey wolf pack. It calculates the fitness values of individual populations separately, and labels the grey wolf level based on the fitness size. Grey wolf α is the leader of all wolf packs, which is responsible for commanding activities such as hunting, gathering, and escaping. Grey wolf β is responsible for assisting grey wolf α in decision-making, supervising and leading other groups to implement actions, and providing feedback on suggested information to grey wolf α . Grey wolf δ and ω are responsible for obeying and executing orders, safeguarding the safety of the wolf pack, and ensuring the balance within the grey wolf pack. The hierarchical system and hunting mechanism of grey wolves are shown in Figure 4 [27-28].

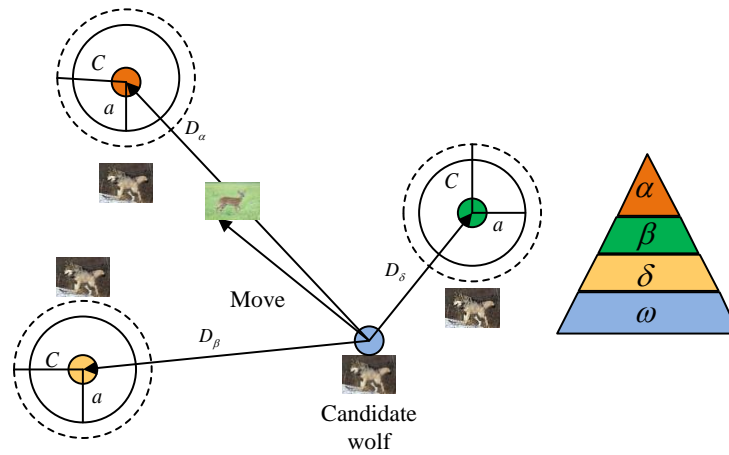


Figure 4: Grey wolf hierarchy and hunting mechanisms

As shown in Figure 4, the population system of grey wolves takes a pivotal part in the hunting process. Grey wolves search and track their prey through group activities, and then surround them from different directions. Grey wolf α commands grey wolf β and δ to launch an attack on their prey, while grey wolf ω is responsible for containment, achieving the transformation and movement of the entire encirclement. The process of the group surrounding the prey is shown in equation (6), wherein D indicates the distance between the grey wolf and the prey. C represents a constant, oscillation factor. $X_{p(t)}, X(t)$ represents the positions of prey and grey wolf at the t iteration.

$$D = |C \cdot X_{p(t)} - X(t)| \tag{6}$$

The calculation of the oscillation factor C is indicated in equation (7), where r_2 represents a random constant between [0,1].

$$C = 2r_2 \tag{7}$$

The position update of the grey wolf is indicated in equation (8), where A represents the convergence factor.

$$X(t+1) = X_p(t) - A \cdot D \tag{8}$$

The calculation of the convergence factor is indicated in equation (9), where a represents a linear decrease from 2 to 0 as the iterations rises. Max_it represents the max number of iterations set. r_1

represents a random constant between [0,1].

$$\begin{cases} A = 2ar_1 - a \\ a = 2 - 2 \frac{t}{Max_it} \end{cases} \tag{9}$$

The hunting phase involves updating the position of ω using the positions of grey wolf α , β , and δ , and the updating process of ω is denoted in Equation (10).

$$\begin{cases} D_\alpha = |C_1 \cdot X_{\alpha(t)} - X(t)| \\ D_\beta = |C_2 \cdot X_{\beta(t)} - X(t)| \\ D_\delta = |C_3 \cdot X_{\delta(t)} - X(t)| \end{cases} \tag{10}$$

The position vectors of wolf packs of different levels are calculated as denoted in equation (11).

$$\begin{cases} X_1 = X_\alpha - A_1 \cdot D_\alpha \\ X_2 = X_\beta - A_2 \cdot D_\beta \\ X_3 = X_\delta - A_3 \cdot D_\delta \end{cases} \tag{11}$$

Equations (10) and (11) can be used to calculate the distance between an individual and the optimal three wolves, and thus comprehensively determine the direction in which the individual moves towards the prey. It implements local or global search based on the size of the convergence factor. The process of optimizing LSTM model parameters using GWO is shown in Figure 5.

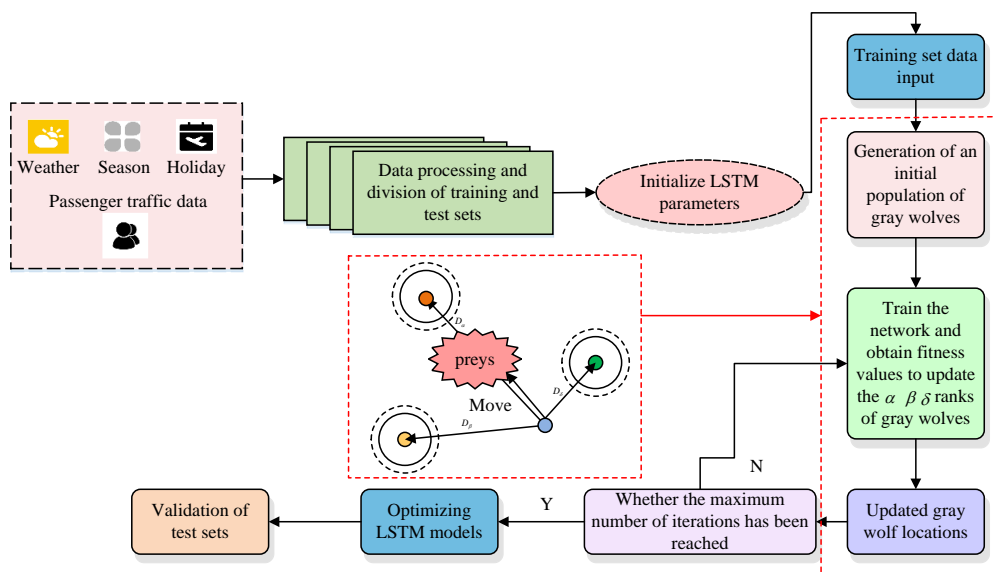


Figure 5: Schematic diagram of the process of optimizing LSTM model parameters by GWO

Although GWO has many advantages and achieves hyperparameter optimization of LSTM models, the GWO algorithm is inclined to get stuck in local optima in the later phrase of parameter optimization. Therefore, the DE algorithm is introduced to optimize the GWO algorithm in this study. DE is an evolutionary algorithm with fast convergence speed and high accuracy, which utilizes the differences between individuals in the population to explore the search space and search for the optimal

solution. The DE algorithm originates from the improvement of genetic annealing algorithm. The algorithm gradually promotes the individuals in the population through continuous iteration, making them gradually approach the optimal solution. The working mechanism of the DE algorithm is indicated in Figure 6 [29-30].

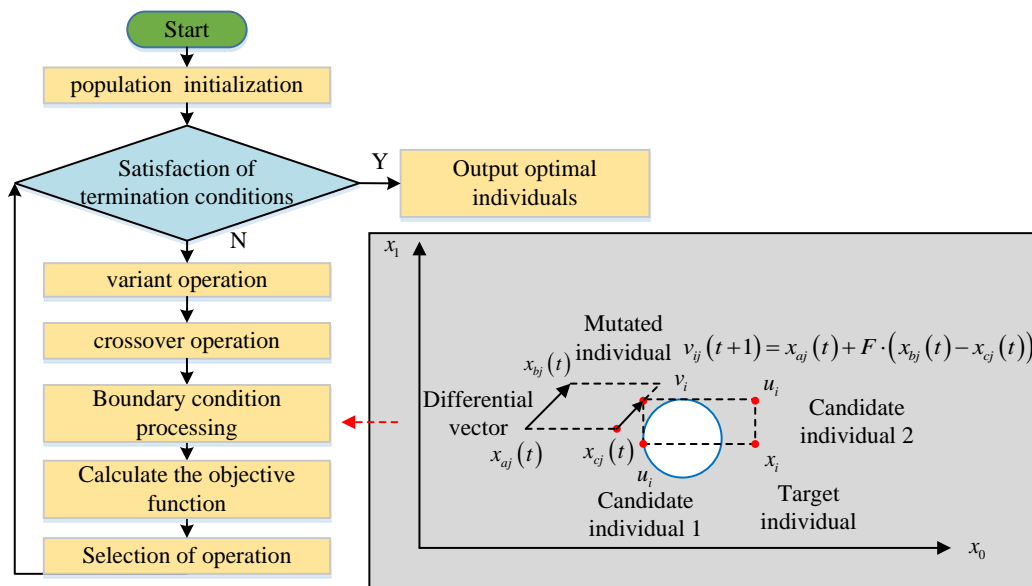


Figure 6: Differential evolution algorithm working mechanism and flow

Firstly, a certain number of individuals are produced as the initial population, and the expression for each individual is shown in equation (12). In equation (12), the i th individual of the population is represented as $x_i(t) = \{x_{i1}(t), x_{i2}(t), \dots, x_{ij}(t), \dots, x_{iD}(t)\}$, where j

represents the parameter index and $j = \{1, 2, \dots, D\}$. x_j^{low}, x_j^{up} represent the boundary conditions of individual population. t represents evolutionary algebra.

$$x_{ij}(0) = x_j^{low} + rand[0,1] \cdot (x_j^{up} - x_j^{low}) \quad (12)$$

The population dominant individuals are calculated based on the fitness function, and then mutation operations are performed within the individuals [31]. New individuals are generated from three individuals through differential strategy, and the calculation is denoted in equation (13). In equation (13), $v_{ij}(t)$ represents the mutated individual. $x_{aj}(t)$, $x_{bj}(t)$, and $x_{cj}(t)$ are three different individuals. $x_{cj}(t)$ stands for mutation operator.

$$v_{ij}(t+1) = x_{aj}(t) + F \cdot (x_{bj}(t) - x_{cj}(t)) \quad (13)$$

In the process of evolution, to increase the diversity of the population, new individuals are crossed with existing individuals, as shown in equation (14). In equation (14), $u_{ij}(t+1)$ represents the variable of variation. C_R represents the crossover operator. j_{rand} represents a random dimension.

$$u_{ij}(t+1) = \begin{cases} v_{ij}(t+1) & \text{if } rand(0,1) \leq C_R \text{ or } j = j_{rand} \\ x_{ij}(t) & \text{if } rand(0,1) > C_R \text{ or } j \neq j_{rand} \end{cases} \quad (14)$$

Finally, the selection operation is conducted according to the greedy criterion, and the calculation process is shown in equation (15) [32]. In equation (15), f represents the fitness function.

$$x_i(t+1) = \begin{cases} u_i(t+1) & \text{if } f(u_i(t+1)) \leq f(x_i(t)) \\ x_i(t) & \text{if } f(u_i(t+1)) > f(x_i(t)) \end{cases} \quad (15)$$

After completing the encirclement, hunting, and attack behavior of the grey wolf population according to the GWO algorithm, the DE algorithm is applied to search for the best wolf location, complete the wolf pack location update, and make the GWO algorithm jump out of the local optimal solution. The process of improving the GWO algorithm by mixing the DE algorithm is shown in Figure 7.

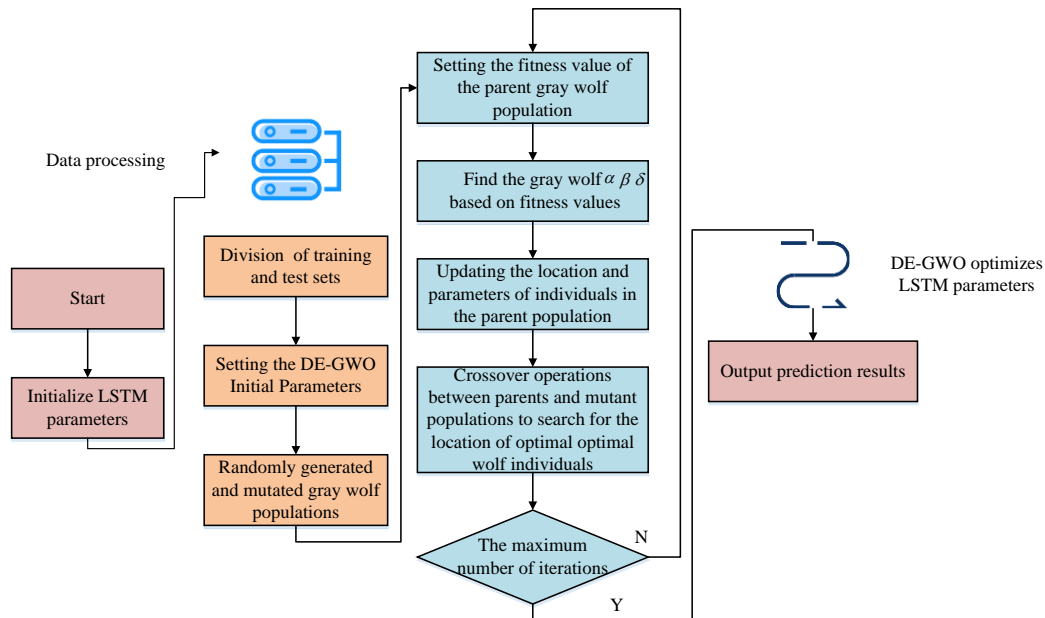


Figure 7: Flowchart of DE algorithm mixed with improved GWO algorithm

4 Performance testing and application effect analysis of tourism passenger flow prediction model

To identify the performance of the hybrid improved GWO algorithm and DE-GWO-LSTM PFP model designed in the research, a series of performance testing experiments and prediction application effect analysis experiments were conducted.

4.1 Performance testing of improved GWO parameter optimization algorithm

Theoretical analysis can to some extent demonstrate the global search capability of the DE hybrid improved GWO algorithm, but quantitative performance analysis is still needed. The performance of the study was validated using different testing functions. The study selected 5 sets of testing functions, namely the unimodal benchmark testing functions Sphere, Quartic, multimodal Rastigin, Ackley, and Generalized Penalized testing functions. Fire-fly Algorithm (FA), Whale Optimization Algorithm (WOA), and traditional GWO were selected for comparison. It set the max number of iterations for the experiment to 1000, the initial population size to 60, and

the optimization times for each function to 40. The optimization outcomes for various test functions are indicated in Table 2. In Table 2, for the two unimodal test functions, the average optimization result of DE-GWO was closer to the global minimum value, with values of 6.134E-12 and 6.189E-10, respectively. The standard deviation value was relatively small, and the improved GWO algorithm had better stability than the traditional GWO algorithm and the other two IOAs on the unimodal test function. On three different multimodal test functions,

the partial optimization values of different optimization algorithms increased, but compared to each other, the improved GWO algorithm’s optimization value was still the smallest. In 40 optimization tests, the convergence rate of the improved GWO algorithm reached 100%. The improvement strategy of research design enabled GWO to effectively explore space, avoiding the occurrence of local optima and solving the problem of multimodal test functions having multiple local minima.

Table 2: Comparison of test function optimization results

Test function	Algorithm	Global minimum	Variable dimension	Average convergence value	Convergence times	Standard deviation value
Sphere	FA	0	30	6.156E-3	16	0.5687
	WOA	0	30	2.371E-5	18	0.2671
	GWO	0	30	7.684E-6	26	0.0061
	DE-GWO	0	30	6.134E-12	40	0.0001
Quartic	FA	0	10	2.644E-4	20	0.6412
	WOA	0	10	6.157E-3	19	0.3941
	GWO	0	10	4.198E-6	23	0.0267
	DE-GWO	0	10	6.189E-10	40	0.0035
Rastrigin	FA	0	10	4.197E-3	13	0.7616
	WOA	0	10	1.684E-5	18	0.7613
	GWO	0	10	6.167E-4	26	0.0646
	DE-GWO	0	10	8.168E-9	40	0.0000
Ackley	FA	0	10	6.164E-2	16	0.6971
	WOA	0	10	1.649E-4	21	0.7364
	GWO	0	10	5.167E-5	33	0.3764
	DE-GWO	0	10	6.169E-7	40	0.0046
Generalized Penalized	FA	0	10	1.649E-2	23	0.6791
	WOA	0	10	1.174E-3	24	0.5314
	GWO	0	10	3.197E-4	29	0.3181
	DE-GWO	0	10	6.318E-6	40	0.0364

The GWO algorithm’s optimization ability before and after improvement was compared and analyzed, population fitness was utilized as the evaluation indicator, and the analysis outcomes are indicated in Figure 8. In Figure 8 (a), the traditional GWO algorithm had a faster evolutionary speed in the early phrase and a slower evolutionary speed in the later phrase. It gradually converged in the middle and later phrases of iteration, approaching the optimal population fitness around 115

generations. In Figure 8 (b), the hybrid optimized DE-GWO algorithm approached the optimal population fitness curve in the early stages of iteration. It can be seen that the DE improvement strategy increased the population fitness ability of the GWO algorithm. With the data analysis in Table 1, the DE-GWO algorithm’s the global optimal solution search ability significantly improved.

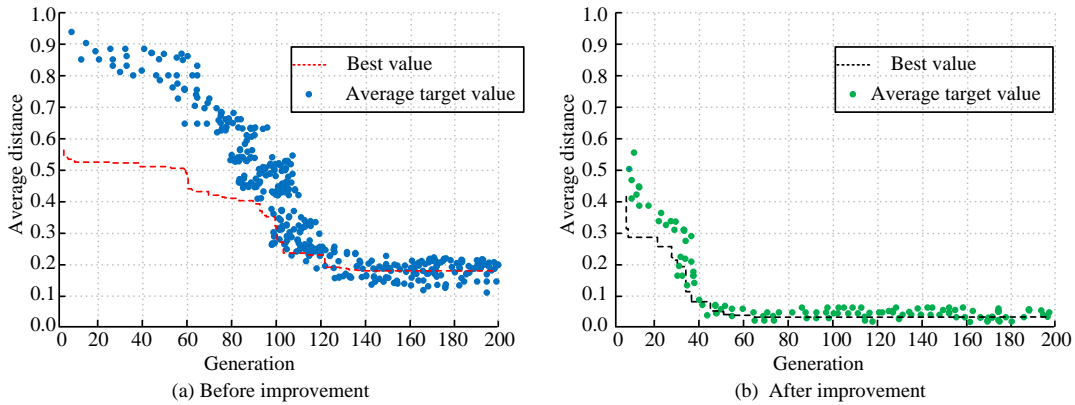


Figure 8: Comparison of population evolution before and after GWO algorithm improvement

4.2 Performance testing of DE-GWO-LSTM prediction model

Firstly, the optimization ability of DE-GWO for LSTM hyperparameters was evaluated, and Hyper volume (HV) and Inverse Generational Distance (IGD) were selected as evaluation indicators. The experiment outcomes are indicated in Figure 9. HV and IGD are convergence indicators for evaluating algorithms. HV can measure the volume occupied by the solution set in the target space. It can be demonstrated that a higher value of HV leads to enhanced performance and convergence of the solution set. IGD measures the distance between the approximate Pareto front generated by the algorithm and the true Pareto front. A reduction in the value of IGD is indicative

of an enhanced convergence of the algorithm. In Figure 9 (a), the HV indicator curve of DE-GWO was the highest, with a maximum value of 0.91. It was better than traditional GWO by 0.74, while the HV value of the FA algorithm was the smallest, only 0.42. As shown in Figure 9 (b), the IGD curve of DE-GWO converged to the minimum value of around 0.09, which was 0.21 lower than the FA algorithm and 0.05 lower than the GWO algorithm. Overall, the DE-GWO algorithm has good convergence in the LSTM parameter optimization process, and the generated Pareto frontier solutions cover a large number of true frontier solutions.

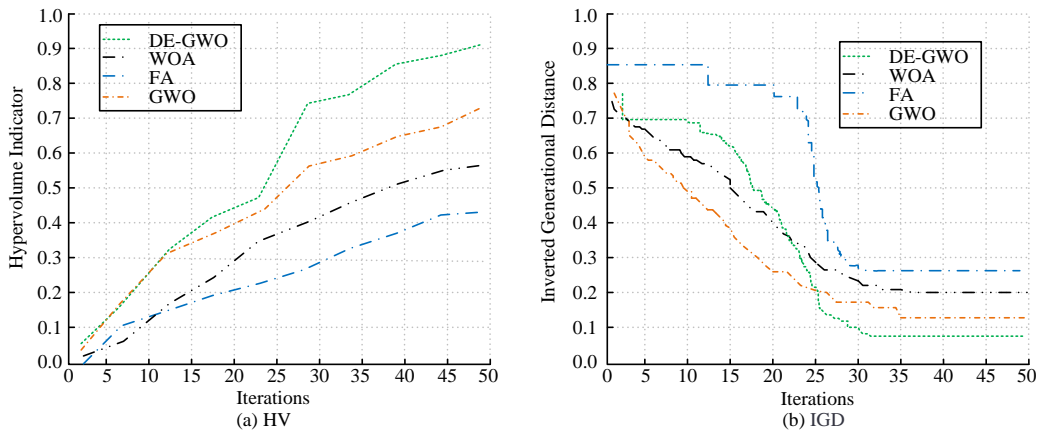


Figure 9: Comparison of HV and IGD for different optimization algorithms

Simultaneously it evaluated the diversity of the solution set of the DE-GWO algorithm, as the diversity of parameters affects the accuracy of the algorithm's prediction. The experimental results of Spacing and Spread are shown in Figure 10. Spacing and Spread indicators measured the minimum and maximum Euclidean distance between all solutions, respectively. The larger the values of the two indicators, the more dispersed and diverse the solutions in the solution set. As shown in Figure 10 (a), the Spacing curve of the

DE-GWO algorithm was at its highest level and ultimately stabilized above the value level of 0.8. As shown in Figure 10 (b), the Spread curve of the DE-GWO algorithm was at the highest level, while the Spread values of the other three algorithms were all below 0.7. The DE-GWO achieved good application results in optimizing LSTM parameters.

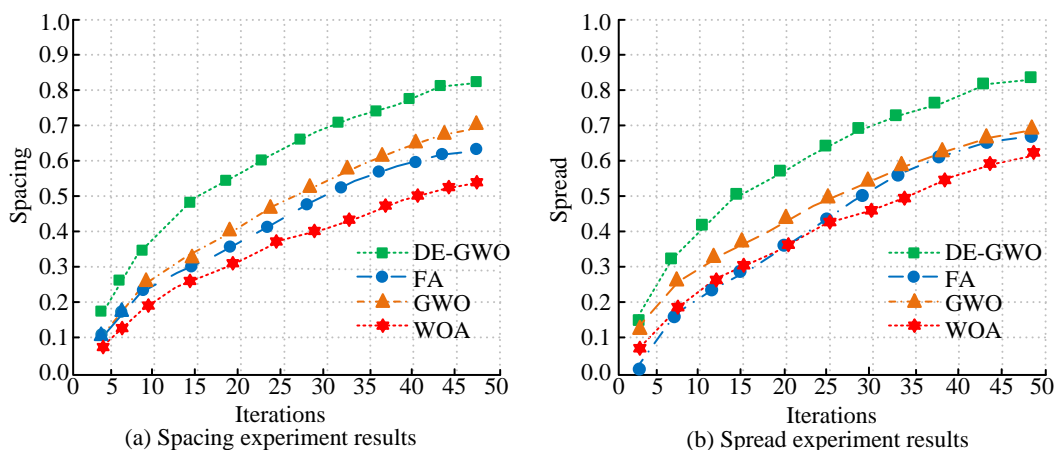


Figure 10: Comparison of solution diversity of different algorithms

Time series prediction models LSTM, GWO-LSTM, and Grey Forecast Model (GM) were selected for performance comparison. The NYC-Taxi, Air-Travel, Public-Transportation, and Retail datasets were utilized as the PFP dataset. NYC-Taxi included the travel records of New York City taxis. Air-Travel contained flight information and passenger data from different airports. Public-Transportation included passenger flow data for public transportation systems such as subways, buses, etc. Retail included both retail store sales records and customer visit records, which can be used for predicting and analyzing traffic in corresponding fields. The experimental data was broken into training and testing sets in an 8:2 ratio.

The MAPE, Root Mean Square Error (RMSE), Mean Absolute Error (MAE), and R2 indicators of different prediction models were compared, and the experiment findings are indicated in Table 3. MAPE, RMSE, and MAE are all indices that determine the deviation between predicted and actual values. The three indices comprehensively assess the model’s predictive ability, and smaller error values indicate better model performance. R2 can measure the degree to which

a predictive model interprets the dependent variable and is applied to evaluate the goodness of fit of the model. The closer the R2 is to 1, the greater the model’s explanatory power for variation in the dependent variable and the better the model’s predictive effectiveness. In Table 3, the three types of error indicators of the improved DE-GWO-LSTM model were the smallest, while those indicators of the traditional LSTM and the GM models had larger values, roughly floating above the 0.4 value level. The performance improvement of the improved GWO-LSTM model was not significant compared to the baseline model, and the error value still fluctuated around 0.3 level. The R2 values of the DE-GWO-LSTM model were all above the 0.85 level, with a maximum value of 0.9450. Compared to traditional LSTM models, it improved by 46.14%. This indicated that the model can accurately fit the characteristics of historical data and use data features at different time scales to complete data prediction. Overall, it can be seen that parameter optimization helped the grey wolf population break out of local optima, improving prediction accuracy and global search ability.

Table 3: Comparison of predictive performance of different prediction models

Model	NYC-Taxi	Air-Travel	Public-Transportation	Retail
LSTM	MAE	0.4861	0.4012	0.5109
	RMSE	0.4392	0.3694	0.4971
	R ²	0.6466	0.6711	0.7130
	MAPE	0.4316	0.4160	0.3915
GWO-LSTM	MAE	0.3106	0.3067	0.3406
	RMSE	0.2906	0.3941	0.3166
	R ²	0.7169	0.7613	0.7164
	MAPE	0.3641	0.3296	0.3064
GM	MAE	0.4216	0.4613	0.4136
	RMSE	0.4035	0.4067	0.3914
	R ²	0.6812	0.6913	0.7066
	MAPE	0.3916	0.4036	0.4162
DE-GWO-LSTM	MAE	0.0693	0.0946	0.1067
	RMSE	0.1306	0.1649	0.1741
	R ²	0.9450	0.9426	0.8697
	MAPE	0.1642	0.0952	0.2234

The results of the time efficiency comparison of different prediction models are shown in Figure 11. In Fig. 11, the prediction efficiency of different prediction models on different datasets was significantly different, but the computational efficiency of DE-GWO-LSTM model was higher in all datasets, indicating that the

hyperparameter seeking optimization of LSTM by GWO algorithm after optimization by DE algorithm improved the efficiency of prediction model, which is comparable to the prediction time of simple baseline model.

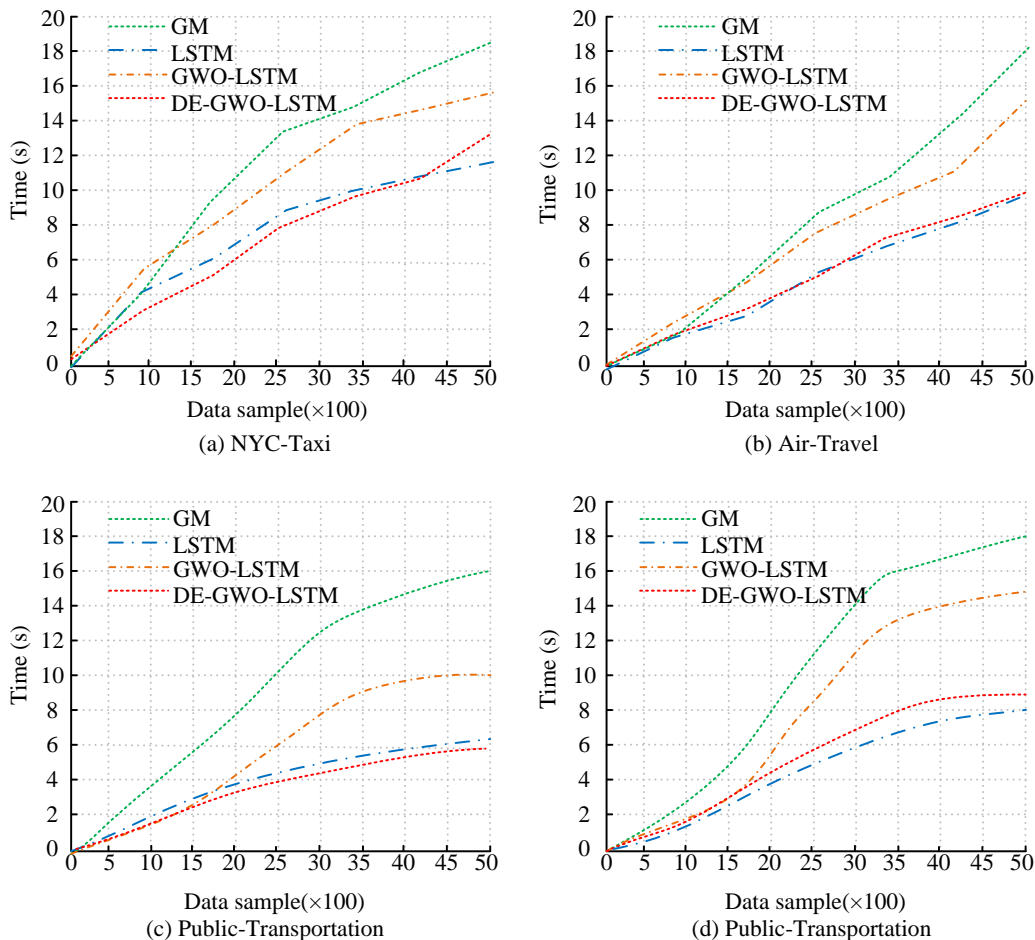


Figure 11: Comparison of prediction efficiency of different models

4.3 Analysis of the application effect of DE-GWO-LSTM passenger flow prediction model

Relevant data of a TA in China from January 1, 2023 to December 31, 2023 was selected as the experimental dataset, with the data from January 1, 2023 to May 31, 2023 as the training set. The data was divided into weekdays and holidays. The prediction results of different time periods and overall is denoted in Figure 12. From sub-figures 12 (a) and (b), the prediction model

designed in the study had a generally consistent trend with the fluctuation of actual passenger flow data for weekdays and holidays, but there were errors in estimating the number of passenger flows at some times. From Figure 12 (c), the prediction model designed in the study was more accurate in predicting the overall passenger flow over a six-month period, with a higher accuracy in predicting the trend of passenger flow and the number of passengers.

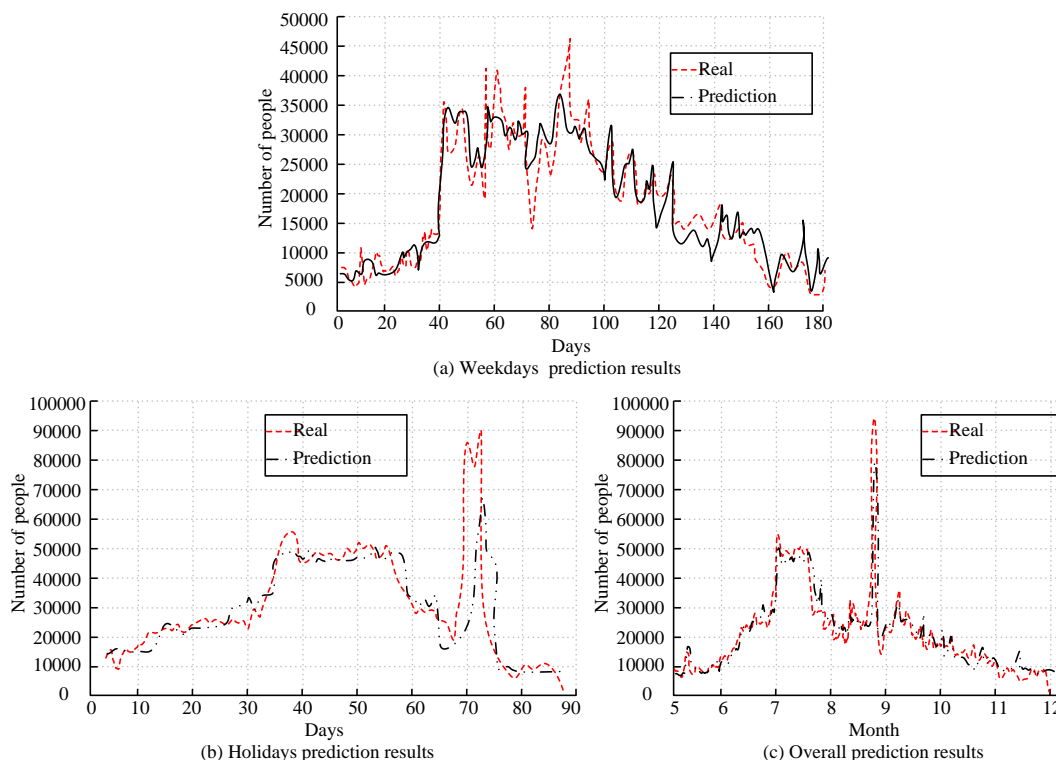


Figure 12: Passenger flow prediction results for different time periods

The accuracy, precision, recall, F1 values, and error stability of the prediction model on the training and testing sets were evaluated and analyzed. The experiment outcomes are indicated in Figure 13. From Figures 13 (a) and (b), those values of the DE-GWO-LSTM prediction model were relatively close on the test and training sets, with an accuracy close to 0.95 and a precision and recall higher than 0.90. The combined use of four indicators comprehensively evaluated the prediction model’s overall effectiveness, meeting the actual needs of tourist flow

prediction in scenic areas. As shown in Figure 13 (c), the model had good predictive stability. The prediction error for different data samples always maintained a relatively stable small range fluctuation, with a stability higher than 0.90. This indicated that the model can accurately predict passenger flow by capturing seasonal and cyclical fluctuations.

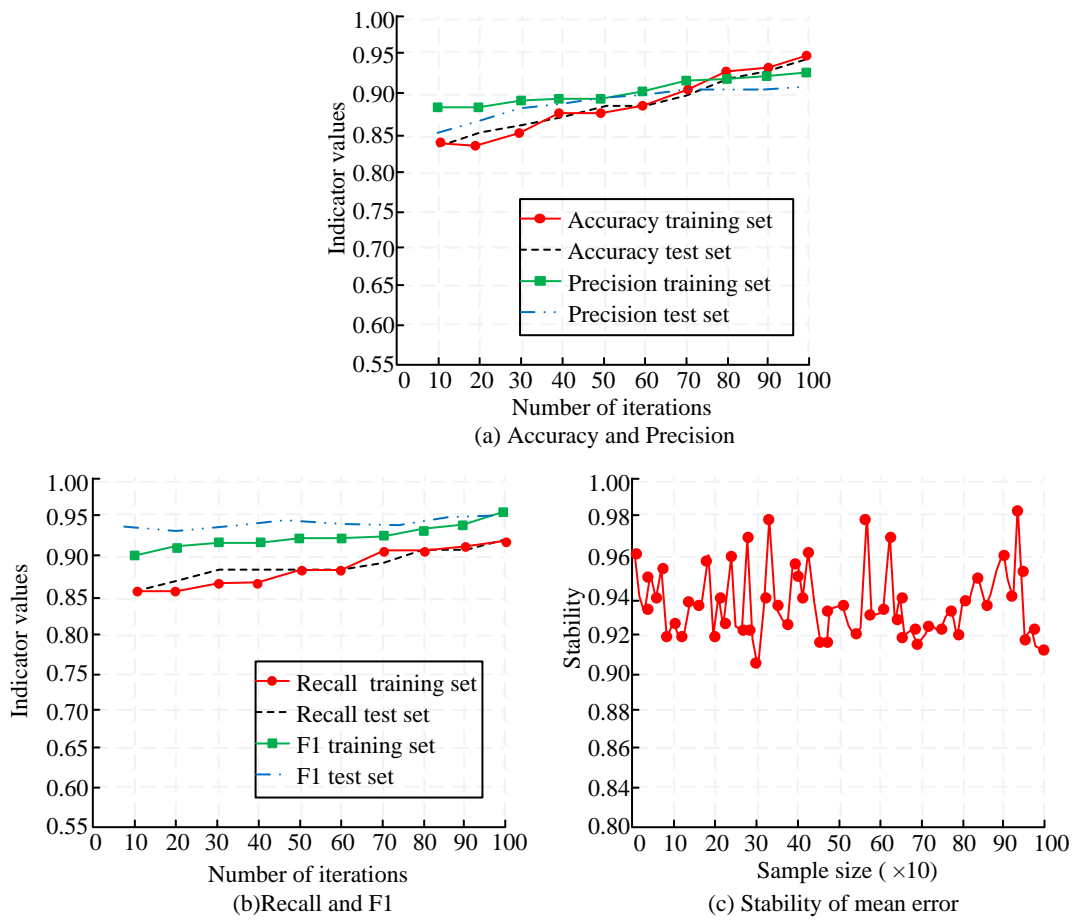


Figure 13: Comprehensive performance evaluation of the prediction model

Finally, the PFP model designed for the study was applied to the simulation of TAs. A questionnaire survey was conducted to analyze and evaluate the economic and social benefits, management convenience, and tourist experience of the prediction model. Quarterly evaluation and follow-up would be conducted, and the statistical outcomes are indicated in Figure 14. As shown in Figure 14, during the follow-up period on a quarterly basis, the satisfaction rating curves of the three stakeholders

towards the predictive model showed an upward trend, achieving good application feedback. This model greatly facilitated the management of scenic spots and prepared tourists' reception scientifically and reasonably based on the predicted results. At the same time, it maximized the travel experience for tourists.

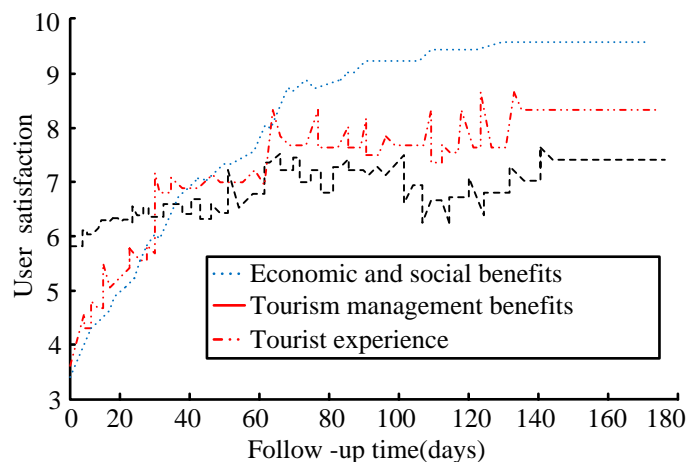


Figure 14: Satisfaction evaluation of predictive model application

5 Discussion

With the continuous development of social economy, empowering the tourism industry through smart tourism is of crucial significance for developing new quality productivity, accelerating the construction of a strong tourism country, and promoting the high-quality development of tourism. To accelerate the development of smart tourism, the study analyzed around the TAs PFP, and the study chose LSTM, which is more sensitive to spatiotemporal sequences, as the basic framework of the prediction model, which is consistent with the technical basis of the literature [12], [18].

At the same time, the study, in the summary of related work, found that the IOA in the process of hyper-parameter optimization to improve the performance of the prediction model was more obvious. Literature [16] uses multi-objective marine predator combination strategy to optimize wind speed prediction, literature [17] uses PSO, Drosophila optimization, lion swarm optimization and SSA to enhance backpropagation neural network, and literature [18] uses flock optimization algorithm to improve bidirectional LSTM prediction model all effectively improve the prediction accuracy. In view of this, the study chose the simpler GWO algorithm to optimize the hyperparameters of LSTM, but the GWO algorithm had the deficiency of easily falling into the local optimum. The study reintroduces the DE algorithm to optimize the population of GWO algorithm, increase the diversity of the population, and improve the algorithm's ability of finding the optimal solution. Compared with the existing advanced research, the study integrated a variety of networks and algorithms to improve the performance of the prediction model, and at the same time, the model complexity was taken into account, and a simpler IOA was introduced, which is a better technical strategy. Comparing the experimental results of the literature [11], it is found that the model designed by the study improves the F1 value by 0.25, and the MAPE takes the lowest value of 0.0952, which is comparable to the results of the literature [14], but the model complexity has been significantly reduced. However, the research integrated LSTM, GWO and DE algorithms to a certain extent also increased the technical complexity, which increased the difficulty of using the technology for the tourism industry.

On the whole, the method designed by the study realizes the optimal combination of DE and GWO, gives full play to the advantages of the two algorithms, and improves the accuracy and efficiency of PFP. This helps to enrich the theoretical research of IOAs and depth studies, and promote the application and development of optimization algorithms in the field of time series forecasting. The use of this method can help scenic spot managers to develop a reasonable resource allocation plan, improve service quality, and optimize the visitor

experience. In future research work, further optimization of the algorithm can be considered to improve the scalability of the model in the face of different sizes of datasets and different types of TAs. Consideration should also be given to realizing further extensions of the forecasting method to increase the applicability of the method in other time series forecasting problems, such as weather forecasting, stock forecasting, and so on. Moreover, the prediction algorithm is integrated using a distributed system in order to realize the real-time prediction of tourist volume.

6 Conclusion

To improve the intelligent and information-based development of tourism and provide tourists with more convenient and personalized travel experiences, an LSTM PFP model improved by introducing IOAs was studied and designed. The experimental results showed that the quantitative analysis results further validated the theoretical analysis. The average optimization results of the unimodal test function were 6.134E-12 and 6.189E-10, respectively, which are closest to the global mini value. The DE algorithm optimized the global search capability of GWO, avoiding the problem of multiple local minima in multimodal test functions. Simultaneously it optimized the grey wolf population's the fitness curve. DE-GWO showed good optimization results for LSTM hyperparameters, with a maximum HV index of 0.91, which is better than the traditional GWO's 0.74. The IGD curve converged to the minimum value of 0.09, a decrease of 0.05 compared to the GWO algorithm. The Spacing and Spread curves were both above the 0.8 value level, indicating better diversity in the solution set. The three error indicators of the DE-GWO-LSTM model on different datasets were the smallest, and the R2 value increased by up to 46.14%. This model had a relatively accurate prediction of overall passenger flow, with good stability in accuracy, precision, recall, and F1 values on the test and training sets. The prediction error fluctuation was small, and it achieved good economic and social benefits, which is conducive to scenic area management and improves the travel experience of tourists. This study is conducive to the intelligent management of tourism, but the accuracy of the prediction model in predicting sudden changes in passenger flow at peaks or valleys still needs to be strengthened.

References

- [1] Junfeng Kang, Xingyu Guo, Lei Fang, Xiangrong Wang, and Zhengqiu Fan. Integration of Internet search data to predict tourism trends using spatial-temporal XGBoost composite model. *International journal of geographical information science*, 36(2):236-252, 2022. <https://doi.org/10.1080/13658816.2021.1934476>
- [2] Jian-Wu Bi, Chunxiao Li, Hong Xu, and Hui Li. Forecasting daily tourism demand for tourist

- attractions with big data: an ensemble deep learning method. *Journal of travel research*, 61(8):1719-1737, 2022. <https://doi.org/10.1177/004728752110405>
- [3] Xiaoyao Zheng, Baoting Han, and Zhen Ni. Tourism route recommendation based on a multi-objective evolutionary algorithm using two-stage decomposition and pareto layering. *IEEE/CAA journal of automatica sinica*, 10(2):486-500, 2023. <https://doi.org/10.1109/JAS.2023.123219>
- [4] Hanyoung Go, and Myunghwa Kang. Metaverse tourism for sustainable tourism development: tourism agenda 2030. *Tourism review*, 78(2):381-394, 2023. <https://doi.org/10.1108/TR-02-2022-0102>
- [5] Chulmo Koo, Jookyung Kwon, Namho Chung, and Jungkeun Kim. Metaverse tourism: conceptual framework and research propositions. *Current issues in tourism*, 26(20):3268-3274, 2023. <https://doi.org/10.1080/13683500.2022.2122781>
- [6] Graham Miller, and Anna Torres-Delgado. Measuring sustainable tourism: a state of the art review of sustainable tourism indicators. *Journal of sustainable tourism*, 31(7):1483-1496, 2023. <https://doi.org/10.1080/09669582.2023.2213859>
- [7] Dogan Gursoy, Yu Li, and Hakjun Song. ChatGPT and the hospitality and tourism industry: an overview of current trends and future research directions. *Journal of hospitality marketing & management*, 32(5):579-592, 2023. <https://doi.org/10.1080/19368623.2023.2211993>
- [8] Shenghong Wang, Yunyun Yu, Jiaqi Chen, and Jun Liu. Impact of climate change on cherry blossom viewing tourism: analysis and simulation based on Weibo proxy data. *Current issues in method and practice*, 26(5):718-734, 2022. <https://doi.org/10.1080/13683500.2022.2049711>
- [9] Yuan Gao, Yao-Yi Chiang, Xiaoxi Zhang, and Min Zhang. Traffic volume prediction for scenic spots based on multi-source and heterogeneous data. *Transactions in GIS*, 26(6):2415-2439, 2022. <https://doi.org/10.1111/tgis.12975>
- [10] Wanying Li, Hongzhi Guan, Yan Han, Haiyan Zhu, and Ange Wang. Short-term holiday travel demand prediction for urban tour transportation: a combined model based on STC-LSTM deep learning approach. *KSCE journal of civil engineering*, 26(9):4086-4102, 2022. <https://doi.org/10.1007/s12205-022-2051-8>
- [11] Fernando Terroso Sáenz, Francisco Arcas-Tunez, and Andres Muñoz. Nation-wide touristic flow prediction with graph neural networks and heterogeneous open data. *Information fusion*, 91(3):582-597, 2023. <https://doi.org/10.1016/j.inffus.2022.11.005>
- [12] Qian Xu. Incorporating CNN-LSTM and SVM with wavelet transform methods for tourist passenger flow prediction. *Soft comput*, 28(3):2719-2736, 2024. <https://doi.org/10.1007/s00500-023-09592-w>
- [13] Gang Xue, Shifeng Liu, Long Ren, and Daqing Gong. Forecasting hourly attraction tourist volume with search engine and social media data for decision support. *Information processing & management*, 60(4):103399-103416, 2023. <https://doi.org/10.1016/j.ipm.2023.103399>
- [14] Haodong Sun, Yang Yang, Yanyan Chen, Xiaoming Liu, and Jiachen Wang. Tourism demand forecasting of multi-attractions with spatiotemporal grid: a convolutional block attention module model. *Information technology & tourism*, 25(2):205-233, 2023. <https://doi.org/10.1007/s40558-023-00247-y>
- [15] Dechun Lu, Yiding Ma, Fanchao Kong, Caixia Guo, Jinbo Miao, and Xiuli Du. Support vector regression with heuristic optimization algorithms for predicting the ground surface displacement induced by EPB shield tunneling. *Gondwana research*, 123(11):3-15, 2023. <https://doi.org/10.1016/j.gr.2022.07.002>
- [16] Jianzhou Wang, Honggang Guo, Zhiwu Li, Aiyi Song, and Xinsong Niu. Quantile deep learning model and multi-objective opposition elite marine predator optimization algorithm for wind speed prediction. *Applied mathematical modelling*, 115(3):56-79, 2023. <https://doi.org/10.1016/j.apm.2022.10.052>
- [17] Xiancheng Mei, Chuanqi Li, Qian Sheng, Zhen Cui, Jian Zhou, and Daniel Dias. Development of a hybrid artificial intelligence model to predict the uniaxial compressive strength of a new aseismic layer made of rubber-sand concrete. *Mechanics of advanced materials and structures*, 30(11):2185-2202, 2023. <https://doi.org/10.1080/15376494.2022.2051780>
- [18] Ilyos Abdullaev, Natalia Prodanova, Mohammed Altaf Ahmed, E. Laxmi Lydia, Bhanu Shrestha, Gyanendra Prasad Joshi, and Woong Cho. Leveraging metaheuristics with artificial intelligence for customer churn prediction in telecom industries. *Electron research archive*, 31(8):4443-4458, 2023. <http://www.aimspress.com/journal/ERA>
- [19] Yuanzhou Zheng, Lei Li, Long Qian, Bosheng Cheng, Wenbo Hou, and Yuan Zhuang. Sine-SSA-BP ship trajectory prediction based on chaotic mapping improved sparrow search algorithm. *Sensors-basel*, 23(2):704-722, 2023. <https://doi.org/10.3390/s23020704>
- [20] Faten Khalid Karim, Doaa Sami Khafaga, Marwa M. Eid, S. K. Towfek, and Hend K. Alkahtani. A novel bio-inspired optimization algorithm design for wind power engineering applications time-series forecasting. *Biomimetics*, 8(3):321-334, 2023. <https://doi.org/10.3390/biomimetics8030321>
- [21] Ejay Nsugbe. Toward a self-supervised architecture for semen quality prediction using environmental and lifestyle factors. *Artificial intelligence and applications*, 1(1):35-42, 2023. <https://orcid.org/0000-0003-0674-1611>

- [22] Tariq Limouni, Reda Yaagoubi, Khalid Bouziane, Khalid Guissi, and El Houssain Baali. Accurate one step and multistep forecasting of very short-term PV power using LSTM-TCN model. *Renewable energy*, 205(4):1010-1024, 2023. <https://doi.org/10.1016/j.renene.2023.01.118>
- [23] Bei Sun, Xudong Liu, Jiayuan Wang, Xuezhe Wei, Hao Yuan, and Haifeng Dai. Short-term performance degradation prediction of a commercial vehicle fuel cell system based on CNN and LSTM hybrid neural network. *International journal of hydrogen energy*, 48(23):8613-8628, 2023. <https://doi.org/10.1016/j.ijhydene.2022.12.005>
- [24] Xia Liu, Kangyi Wang, and Chongguang Liu. Recognition and prediction of nonlinear dynamic states of microelectronic devices based on machine learning algorithms. *Informatica-lithuan*, 48(10):119-132, 2024. <https://doi.org/10.31449/inf.v48i10.6010>
- [25] Irfan Ullah, Kai Liu, Toshiyuki Yamamoto, Md Shafiullah, and Arshad Jamal. Grey wolf optimizer-based machine learning algorithm to predict electric vehicle charging duration time. *Transportation letters*, 15(8):889-906, 2023. <https://doi.org/10.1080/19427867.2022.2111902>
- [26] Hemn Unis Ahmed, Reham R. Mostafa, Ahmed Mohammed, Parveen Sihag, and Azad Qadir. Support vector regression (SVR) and grey wolf optimization (GWO) to predict the compressive strength of GGBFS-based geopolymer concrete. *Neural computing and applications*, 35(3):2909-2926, 2023. <https://doi.org/10.1007/s00521-022-07724-1>
- [27] Osman Altay, and Elif Varol Altay. A novel hybrid multilayer perceptron neural network with improved grey wolf optimizer. *Neural computing and applications*, 35(1):529-556, 2023. <https://doi.org/10.1007/s00521-022-07775-4>
- [28] Zakariya A. Oraibi, and Safaa Albasri. Efficient COVID-19 prediction by merging various deep learning architectures. *Informatica-lithuan*, 48(5):55-62, 2024. <https://doi.org/10.31449/inf.v48i5.5424S>
- [29] Sanjoy Chakraborty, Apu Kumar Saha, Absalom E. Ezugwu, Jeffrey O. Agushaka, Raed Abu Zitar, and Laith Abualigah. Differential evolution and its applications in image processing problems: a comprehensive review. *Archives of computational methods in engineering*, 30(2):985-1040, 2023. <https://doi.org/10.1007/s11831-022-09825-5>
- [30] Anuradha Thakare, Ahmed M. Anter, and Ajith Abraham. Seizure disorders recognition model from EEG signals using new probabilistic particle swarm optimizer and sequential differential evolution. *Multidimensional systems and signal processing*, 34(2):397-421, 2023. <https://doi.org/10.1007/s11045-023-00870-2>
- [31] Hongliang Zhang, Tong Liu, Xiaojia Ye, Ali Asghar Heidari, Guoxi Liang, Huiling Chen, and Zhifang Pan. Differential evolution-assisted salp swarm algorithm with chaotic structure for real-world problems. *Engineering with computers*, 39(3):1735-1769, 2023. <https://doi.org/10.1007/s00366-021-01545-x>
- [32] Manoharan Premkumar, Chandrasekaran Kumar, Thankkapan Dharma Raj, Somasundaram David Thanasingh Sundarsingh Jebaseelan, Pradeep Jangir, and Hassan Haes Alhelou. A reliable optimization framework using ensembled successive history adaptive differential evolutionary algorithm for optimal power flow problems. *The IET generation transmission & distribution*, 17(6):1333-1357, 2023. <https://doi.org/10.1049/gtd2.12738>

